University of Zurich[UZH]

Zurich Open Repository and Archive
University of Zurich
University Library
Strickhofstrasse 39
CH-8057 Zurich
www.zora.uzh.ch

Year: 2010

The large hydrophilic loop of presenilin 1 is important for regulating gamma-secretase complex assembly and dictating the amyloid beta peptide (Abeta) Profile without affecting Notch processing

Wanngren, J ; Frånberg, J ; Svensson, A I ; Laudon, H ; Olsson, F ; Winblad, B ; Liu, F ; Näslund, J ; Lundkvist, J ; Karlström, H

Abstract: Gamma-secretase is an enzyme complex that mediates both Notch signaling and beta-amyloid precursor protein (APP) processing, resulting in the generation of Notch intracellular domain, APP intracellular domain, and the amyloid beta peptide (Abeta), the latter playing a central role in Alzheimer disease (AD). By a hitherto undefined mechanism, the activity of gamma-secretase gives rise to Abeta peptides of different lengths, where Abeta42 is considered to play a particular role in AD. In this study we have examined the role of the large hydrophilic loop (amino acids 320-374, encoded by exon 10) of presenilin 1 (PS1), the catalytic subunit of gamma-secretase, for gamma-secretase complex formation and activity on Notch and APP processing. Deletion of exon 10 resulted in impaired PS1 endoproteolysis, gamma-secretase complex formation, and had a differential effect on Abeta-peptide production. Although the production of Abeta38, Abeta39, and Abeta40 was severely impaired, the effect on Abeta42 was affected to a lesser extent, implying that the production of the AD-related Abeta42 peptide is separate from the production of the Abeta38, Abeta39, and Abeta40 peptides. Interestingly, formation of the intracellular domains of both APP and Notch was intact, implying a differential cleavage activity between the epsilon/S3 and gamma sites. The most C-terminal amino acids of the hydrophilic loop were important for regulating APP processing. In summary, the large hydrophilic loop of PS1 appears to differentially regulate the relative production of different Abeta peptides without affecting Notch processing, two parameters of significance when considering gamma-secretase as a target for pharmaceutical intervention in AD.

DOI: https://doi.org/10.1074/jbc.M109.055590

Posted at the Zurich Open Repository and Archive, University of Zurich
ZORA URL: https://doi.org/10.5167/uzh-42447
Journal Article
Accepted Version

Originally published at:
Wanngren, J; Frånberg, J; Svensson, A I; Laudon, H; Olsson, F; Winblad, B; Liu, F; Näslund, J; Lundkvist, J; Karlström, H (2010). The large hydrophilic loop of presenilin 1 is important for regulating gamma-secretase complex assembly and dictating the amyloid beta peptide (Abeta) Profile without affecting Notch processing. Journal of Biological Chemistry, 285(12):8527-8536.
DOI: https://doi.org/10.1074/jbc.M109.055590

JBC Papers in Press. Published on January 27, 2010 as Manuscript M109.055590
The latest version is at http://www.jbc.org/cgi/doi/10.1074/jbc.M109.055590

THE LARGE HYDROPHILIC LOOP OF PRESENILIN 1 IS IMPORTANT FOR REGULATING γ-SECRETASE COMPLEX ASSEMBLY AND DICTATING THE Aβ PROFILE WITHOUT AFFECTING NOTCH PROCESSING

Johanna Wanngren[1], Jenny Frånberg[1], Annelie I Svensson[1], Hanna Laudon[1], Bengt Winblad[1], Frank Liu[3], Jan Näslund[2], Johan Lundkvist[2] and Helena Karlström[1]

[1]From the Department of Neurobiology, Caring Sciences and Society, KI-Alzheimer Disease Research Center, Karolinska Institutet, Novum, SE-141 86 Stockholm, Sweden

[2]From AstraZeneca CNS/Pain RA, Division of Molecular Pharmacology, Södertälje, Sweden

[3]From AstraZeneca, Division of Neuroscience Biology, Wilmington, Delaware, USA

Running head: PS1 hydrophilic loop affect APP processing

Address correspondence to: Dr. Helena Karlström, Karolinska Institutet, Department of Neurobiology, Caring Sciences and Society, Novum, 5th floor, SE-141 57 Stockholm, Sweden. Fax +46 8 58583645; E-mail: Helena.Karlstrom@ki.se

γ-Secretase is an enzyme complex that mediates both Notch signaling and β-amyloid precursor protein (APP) processing, resulting in the generation of Notch intracellular domain (NICD), APP intracellular domain (AICD) and the amyloid β-peptide (Aβ), the latter playing a central role in Alzheimer's disease (AD). By a hitherto undefined mechanism, the activity of γ-secretase gives rise to Aβ peptides of different lengths, where Aβ42 is considered to play a particular role in AD. In this study we have examined the role of the large hydrophilic loop (amino acids 320-374, encoded by exon 10) of presenilin 1 (PS1), the catalytic subunit of γ-secretase, for γ-secretase complex formation and activity on Notch and APP processing. Deletion of exon 10 resulted in impaired PS1 endoproteolysis, γ-secretase complex formation and had a differential effect on Aβ-peptide production. While the production of Aβ38, Aβ39 and Aβ40 was severely impaired, the effect on Aβ42 was affected to a lesser extent, implying that the production of the AD-related Aβ42 peptide is separate from the production of the Aβ38, Aβ39 and Aβ40 peptides. Interestingly, formation of the intracellular domains of both APP (AICD) and Notch (NICD) was intact, implying a differential cleavage activity between the epsilon/S3 and gamma-sites. The most C-terminal amino acids of the hydrophilic loop were important for regulating APP processing. In summary, the large hydrophilic loop of PS1 appears to differentially regulate the relative production of different Aβ peptides without affecting Notch processing, two parameters of significance when considering γ-secretase as a target for pharmaceutical intervention in AD.

Alzheimer's disease (AD) is the most common form of dementia in elderly and is a multifactorial disease caused by a progressive neurodegeneration, leading to dementia and eventually to death. Neuropathological hallmarks of AD include intracellular neurofibrillary tangles composed of the hyperphosphorylated tau protein and extracellular senile plaques, which are mainly deposits of the amyloid β-peptide (Aβ) (1,2). Aβ is generated from the amyloid precursor protein (APP) by a sequential cleavage of β-secretase (BACE) and γ-secretase (3). Interfering with either β- or γ-secretase activities hold great promise as disease-modifying strategies for AD.

γ-Secretase is a member of a subset of proteases that cleaves its substrate within the membrane, a process that has been named regulated intramembrane proteolysis (RIP) (4). In contrast to other enzymes catalyzing RIP, γ-secretase is a multi-subunit complex composed of four members; presenilin (PS), nicastrin, Pen-2 and Aph-1 (5-8). PS1 plays a central role in the complex since it provides the catalytic core of the complex via Asp-257 and Asp-385, located in transmembrane domains (TMD) 6 and 7, respectively (7). Apart from APP, γ-secretase is also involved in the processing of many other types of Type I transmembrane proteins, most importantly the Notch receptor. Notch is an important signaling molecule in cell differentiation during development but recent studies in adult mice using non-selective γ-secretase inhibitors have revealed its importance during adulthood as well. Perturbations of Notch signaling in adult mice affect cell homeostasis, tissue

Copyright 2010 by The American Society for Biochemistry and Molecular Biology, Inc.

Downloaded from www.jbc.org at SMAC Consortium - University of Zürich, on March 14, 2011

differentiation in lymphocytes, gastrointestinal tracts, pancreas and the skin (9-12).

There are two homologues of PS in humans, PS1 and PS2, which have been characterized as nine TMD proteins (13-15) and share an average homology of 63%, and up to 95% within the TMDs (reviewed in (16)). The PS molecules undergo endoproteolysis upon assembly of all γ-secretase members in the ER and/or early Golgi compartment, generating the active N-terminal and C-terminal fragment (NTF and CTF) (17). The Aβ-peptide produced from γ-secretase-mediated cleavage of APP can be of various lengths, 37-43 amino acids, where the most abundant forms are Aβ40 and Aβ42 (18-20). The Aβ42 peptide is more prone to aggregate and believed to be the toxic form that causes synaptic and neuronal damage in the brain (21). Many studies have recently pointed out the ratio between these C-terminal variants to be of importance for the formation of plaques. For instance many familial Alzheimer's disease mutations (FAD) in PS1 and 2 cause an increase in Aβ42/Aβ40 ratio either by decreasing the production of Aβ40 or by increasing the Aβ42 generation (22,23). This increased ratio is often considered as gain of function of the γ-secretase complex. However, most of the FAD PS mutants have reduced proteolytic activity implying that the mutations are instead loss of function mutations (22-25). Although PS1 and PS2 share a high degree of homology and can form γ-secretase complexes that are both active on APP and Notch processing, there are some domains that differ extensively between these two proteins, especially the large cytoplasmic loop between TMD 6 and 7 (26). These loops are 110 amino acids in length in PS1 and 84 amino acids in length in PS2 and share only 16% homology when performing protein blast alignment (www.blast.nvbi.nlm.nih.gov). It has been shown that the PS1 loop binds to β-catenin and N-cadherin but it has been demonstrated that the β-catenin binding domain is not essential for γ-secretase activity since a PS1 molecule lacking the loop can rescue a PS1 -/- lethal phenotype (27). Moreover, the absence of the large cytoplasmic loop does not influence the increased Aβ42/Aβ40 ratio caused by PS1 and PS2 FAD mutations (28). Recently, however, Deng *et al.* showed that PS1Δexon 10 knock-in mice, which lacks a big portion of the large cytoplasmic loop, had increased amyloid pathology and impaired γ-secretase activity (assessed by accumulation of APP-CTF and reduced Aβ40 formation) (29), indicating a more pronounced functional role for this large domain.

In order to further probe the functional role of the large cytoplasmic loop in PS1, we have investigated this region systematically in cells devoid of both PS1 and PS2.

EXPERIMENTAL PROCEDURES

cDNA constructs- Full-length PS1wt were cloned into the pcDNA5FRT/TO vector (Invitrogen) on BamH1/Not1 sites. The PS1Δexon 10 construct lacks the amino acids 320-374 (PS1 numbering) and was first created by using PCR with the BGH primer and the Δexon 10 Fw primer and the T7 and Δexon 10 Rev primers (Supplementary Data, Table S1), respectively. After a second PCR, the two fragments were linked together using the T7 and BGH primers and the PS1Δexon 10 molecule was cloned into the pcDNAFRT/TO vector on BamH1/Not1 sites. PS1 NTFwt and CTFwt have been described elsewhere (30). The PS1 CTF N-terminal truncated constructs were created by in vitro mutagenesis according to Quick Change mutagenesis protocol (Stratagene) using following primers: CTFcasp (start 345), CTF start 355, CTF start 365 and CTF start 375, see Supplementary Data, Table S1. The mutagenesis was performed on CTFwt mentioned above. For CTF start 375 D385A the same primers were used as for CTF start 375 but the template was CTF D385A, which has also been described elsewhere (30). The CTF molecules were cloned into BamH1/Not1 sites in the pcDNA5FRT/TO vector (Invitrogen). Introduction of the glycosylation acceptor sites on PS1wt and PS1Δexon 10, both in pcDNA5FRT/TO, were performed using the OptC primers (Supplementary Data, Table S1) according to Quick Change mutagenesis protocol (Stratagene). The APPwt in pcDNA3, used for generating a stable cell line, was cloned into the previously described pENTR2B vector (31) on NotI/EcoRV sites and then transferred to the pCAG-IRES-Puro vector using Gateway cloning technology (Invitrogen). The DNA sequence of all constructs was verified using the BigDye®

Downloaded from www.jbc.org at SMAC Consortium - University of Zürich, on March 14, 2011

Terminator v3.1 Cycle Sequencing Kit (Applied Biosystems). The reporter constructs: MH100, CMV-β-gal, C99-GVP and NotchΔE-GVP used in the luciferase-based reporter gene assay have been described previously (32,33).

Cell culture and transfection- Blastocyst-derived embryonic stem cells deficient for PS1 and PS2, BD8 cells (34), were cultured in ES medium; DMEM supplemented with 10% fetal calf serum, 1 mM sodium pyruvate, 0.1 mM β-mercaptoethanol and non-essential amino acids (Invitrogen). Flp-In-BD8 cells, established elsewhere (26), stably expressing APPwt in pcDNA3.1 (BD8:APP) were generated by transfection following maintenance in media supplemented with puromycin (1 µg/ml) for 2 weeks. Clonal picking and characterization of APP expression was preformed to avoid clonal variation. A clone with high APP expression was chosen for further use in these experiments. The same clone were also used for creating cell lines stably expressing the PS1wt- or PS1Δexon 10- pcDNA5-FRT/TO vectors, generated according to the Flp-In protocol (Invitrogen). Briefly, by co-transfecting a vector containing the gene of interest and an FRT site together with a vector encoding the Flp recombinase this system targets the gene to a specific genomic site. Following transfection, cells were selected by supplementing the medium with hygromycin (750 µg/ml) for 2 weeks. The surviving cells were expanded and further analyzed for their PS1 expression

BD8 cells stably expressing PS1 NTFwt (BD8:NTF) have been previously generated in our laboratory (35). The cDNA constructs were transiently transfected into the BD8, BD8:APP and BD8:NTF using the Lipofectamine2000 reagent (Invitrogen) according to the manufacturer's instructions.

Antibodies for immunoblottning- PS1-NTF (NT-1, a gift from Dr. Paul M. Mathews, Nathan Kline Institute) recognizing the C-terminal loop region of PS1, NCT (N1660, Sigma-Aldrich) raised against C-terminal residues 693-709 of Nicastrin, Pen-2 (3981 ProSci Incorporated) raised against residues 1-13 of Pen-2, Aph-1aL (O2C2, Covance) recognizing the residues 245-265 of Aph-1aL and β-actin (Abcam).

SDS-PAGE and Western blot- Cells were lysed 24-48 hours post transfection in Cell lysis buffert (10 mM Tris pH 8.1, 1 mM EDTA, 150 mM NaCl and 0.65% Nonidet P-40) supplemented with Protease Inhibitor Cocktail (Roche). Protein levels were determined by the BCA™ Protein Assay kit (PIERCE) and equal amount of protein in Laemmli sample buffer (SIGMA) were separated using NuPAGE BIS-Tris pre-cast gradient 4-12% gel and MES buffer (Invitrogen). Proteins were transferred to a nitrocellulose membrane (BioRad) and blocked with 5% dry milk followed by incubation of primary antibody over night at 4 °C. After applying the secondary horseradish peroxidise linked antibodies (1:2000, GE Healthcare) for one hour in room temperature the blots were developed with ECL solution, Immobilon™ Western Chemiluminescent HRP Substrate (Millipore) using Amersham HyperfilmTM ECL (GE Healthcare) or the CCD camera LAS-3000 (FUJIFILM Life Science). In the case of quantification, the respective bands were measured using ImageJ software (NIH).

Co-immunoprecipitation- Co-immunoprecipitation experiments were carried out 48 hours post transfection from BD8 cells grown in 10 cm plates. Cells were harvested in PBS, pelleted and lysed by sonication in 200 µl co-immunoprecipitation buffer containing: 50 mM Hepes pH 7.4, 150 mM NaCl, 2 mM EDTA, 1% CHAPSO and Protease Inhibitor Cocktail (Roche). The samples were kept on ice, and all incubations were performed at 4 °C. The lysate were subjected to ultracentrifugation at 100 000 x g for 20 min, followed by preclearing of the supernatant by 50 µl/ml lysate with a mixture of protein A and protein G sepharose (Amersham). Samples were then incubated with primary antibody diluted 1:250 over night with end-over-end rotation. The Nicastrin antibody N1660 and the Aph-1aL antibody O2C2 were used as primary antibodies or purified rabbit IgG as a negative control. The following day, a mixture of protein A and protein G sepharose was added to the samples and incubated for an additional 1 hour. Next, the precipitates were washed three times with co-immunoprecipitation buffer containing 0.5% CHAPSO and once in PBS. Laemmli sample buffer (SIGMA) was added and incubated at room temperature for 30 min prior to SDS-PAGE and Western blot. The membranes were then analyzed with the NT1, and 3981 antibodies.

Downloaded from www.jbc.org at SMAC Consortium - University of Zürich, on March 14, 2011

GCB pulldown- To analyze the presence of active γ-secretase complexes, BD8 cells stably expressing PS1wt- or PS1Δexon 10 were subjected to GCB pulldown. GCB is composed of the γ -secretase inhibitor L685,458 and a biotin group separated by a long cleavable hydrophilic linker. The GCB pulldown, its structure and characteristics have been described previously (36). Briefly, membrane preparations of the cells were dissolved in 0.5% CHAPSO and protein levels were determined by the BCA™ Protein Assay kit (PIERCE) before the GCB pulldown. The specificity of the pulldown was confirmed by the addition of excess amounts of competing non-biotinylated L685,458. The captured γ-secretase components were eluted, subjected to SDS-PAGE and Western blot and analyzed with the NT1 antibody.

Endoglycosidase H treatment- BD8 cells transiently transfected with PS1wt, PS1wt optC, PS1Δexon 10 or PS1Δexon 10 optC in 6-well tissue culture plates were harvested 24 hours post-transfection. The Endoglycosidase H treatment has been described elsewhere (37). Protein levels were determined by the BCA™ Protein Assay kit (PIERCE) and next the samples were subjected to SDS-PAGE and Western blot and then analyzed with the NT1 antibody.

Determination of the endoproteolytic pattern of the PS1Δexon 10 molecule- The endoproteolysis pattern of the PS1Δexon 10 molecule was analyzed from seven membranes by quantifying the intensity of the full-length, FL, and the NTF band of PS1wt and PS1Δexon 10 in the CCD camera. Next, the ratio of NTF/FL were calculated and compared to the ratio for the PS1wt.

Luciferase reporter gene assay- BD8 cells were transfected using a total amount of 1500 ng DNA consisting of: 300 ng PS1wt/ PS1Δexon 10 or 300 ng of each NTFwt and truncated CTF, empty pcDNA5 vector was also added to adjust of difference in DNA amounts. Further, 300 ng MH100, 200 ng CMV-β-gal, 100 ng GFP and 300 ng C99-GVP/NotchΔE-GVP were added. Cells were lysed 36 hours post transfection and then analyzed as previously described (33). To adjust for differences in transfection efficiency, the β -galactosidase activity of the cell lysate was determined. The luciferase activity was also normalized for protein expression using a PS1-NTF antibody (NT-1). Experiments were performed in triplicates and repeated 4-5 times.

Quantification of secreted Aβ- A sandwich immunoassay using the Meso Scale Discovery Sector Imager 6000 was used to quantify secreted Aβ peptides in conditioned medium. All reagents were from Meso Scale Discovery, if not stated otherwise. BD8:APP were transfected with 800ng PS1wt/ PS1Δexon 10 or 800ng of each NTFwt and truncated CTF, empty pcDNA5 vector was added to adjust for differences in DNA amounts, 200 ng CMV-β-gal and 100 ng GFP. Next, cells were incubated in 240 µl of fresh ES medium containing either 1 µM L685,458 or vehicle (DMSO) for 36 hours before analysis of the conditioned medium. Multi-Array plates pre-coated with either Triplex C-terminal specific anti-Aβ40/38/42 antibodies or 6E10 were blocked and washed according to manufacturer's instructions. Media samples and Aβ peptide standards (Meso Scale Discovery and AnaSpec) as well as a ruthenylated- 6E10 or C-terminal specific anti-Aβ42 (SULFO-TAG™) detection antibodies, or primary anti-Aβ40 and anti-Aβ39 antibodies (both from AstraZeneca), were added to the samples before incubation at 4°C over night. Next day, the 6E10 pre-coated plates with primary anti-Aβ40 or anti-Aβ39 antibodies were subjected to a secondary ruthenylated-anti-rabbit (SULFO-TAG™) antibody. For total Aβ detection, samples were incubated over night and then subjected to ruthenylated-4G8 (SULFO-TAG™) at room temperature for 2 hours, before all plates were washed. All antibodies were diluted in 1% blocking buffer. For detection, Meso Scale Discovery Read buffer was added and the light emission at 620 nm was measured after electrochemical stimulation. The corresponding concentrations of Aβ peptides in the samples were calculated using the Aβ peptide standard curves. Next, the β-galactosidase activity of the cell lysate was determined, to adjust for differences in transfection efficiency. The secreted Aβ40 peptide was also normalized for protein expression using a PS1-NTF antibody (NT-1). Experiments were performed in triplicates or duplicates and repeated 4-6 times.

Cycloheximide treatment of cells- BD8 and BD8:NTF cells were transfected in one well of a 6 well tissue-culture plate with 500 ng CMV-β-gal and 200 ng GFP as well as 2000 ng

Downloaded from www.jbc.org at SMAC Consortium - University of Zürich, on March 14, 2011

PS1wt or PS1Δexon 10 for BD8 cells or 2000 ng each of CTFwt or CTF start 375 for BD8:NTF. 6 hours post transfection, the cells were divided to 8 wells and incubated for 36 hours. Transfected cells were exposed to 50 µg/ml cycloheximide for 0, 0.5, 1, 2, 4, 8, 12 and 16 hours and then lysed in 200 µl Whole cell extraction buffer (20 mM HEPES pH 7.8, 0.42 M NaCl, 0.5% NP40, 25% glycerol, 0.2 mM EDTA, 1.5 mM $MgCl_2$, 1 mM DTT) supplemented with Protease Inhibitor Cocktail (Roche) for 30 min at 4 °C. Protein levels were determined by the BCA™ Protein Assay kit (PIERCE) and equal amount of protein from the cell extracts from the T=0 time-point was analyzed for full-length PS1 and/or PS1 NTF expression by SDS-PAGE and immunoblottning using the NT1 antibody. β-galactosidase measurements was done, as described above, to ensure equal transfection efficiency After quantifying the intensity with the CCD camera, protein levels for the different constructs were correlated to the construct showing the lowest expression, i.e. PS1wt vs. PS1Δexon 10 and CTFwt vs. the CTF start 375. Proteins from various time points for each construct were separated by SDS-PAGE on 4-12% Bis-Tris gels and analyzed as above. The same blots were also stained with anti-β-actin antibody to ensure for equal amounts of loaded protein. The experiment was repeated three times.

Statistics- All experiments in this paper were performed at least three times in duplicates or triplicates. The non-parametric Mann-Whitney U test by the STATISTICA 8 software from StatSoft was used for statistical analysis.

RESULTS

Metabolism and topology of PS1 lacking exon 10. Although the large hydrophilic loop in PS1 has been suggested to be dispensable for γ-secretase activity (27,28) we wanted to further explore the altered Aβ generation observed in a knock-in mouse model lacking a big portion of this loop (29). To address this we have used cells deficient for PS1 and PS2 (BD8), to nullify the influence from endogenous PS, thereby simplifying interpretation of results. We constructed a cDNA that encodes the human PS1 protein without the loop region (Δ320-374), termed PS1Δexon 10 (Fig. 1A). Since the endoproteolytic site is still present in the construct (Met292) (38,39), we did not expect to disrupt this cleavage event. Indeed, a 30-kDa PS1Δexon 10 derived NTF, which co-migrated with NTF derived from full-length, FL, PS1wt was observed when these constructs were transfected into BD8 cells (Fig. 1B). As expected, the "full-length" PS1Δexon 10 also migrated faster on the gel compared to full-length PS1wt due to the deletion of 55 amino acids a in the loop (Fig. 1B).

To investigate if PS1Δexon 10 could form γ-secretase complexes we performed co-immunoprecipitation studies under conditions preserving complex integrity. By using two different capture antibodies, we showed that the PS1Δexon 10 molecule interacted with nicastrin, Aph-1 and Pen-2 (Fig. 1C). In addition, by using GCB pulldown, we confirmed that an active site directed transition state analogue inhibitor of γ-secretase binds to the PS1-NTF of the PS1Δexon 10 molecule (Fig. 1D). This demonstrates that PS1Δexon 10 can assemble into a bona fide authentic and active γ-secretase complex. However, we observed a tendency of decreased binding of PS1Δexon10 compared to PS1wt (15-70% reduction, three independent experiments) to the inhibitor (the ratio pulldown NTF/input NTF). This suggests a conformational change of the active site in the PS1Δexon 10 molecule.

Interestingly, we noticed that lower levels of NTF were formed from PS1Δexon 10 compared to PS1wt (Fig. 1B). We therefore compared the endoproteolytic pattern of PS1Δexon 10 to PS1wt. By quantifying the full-length, FL, and the NTF band of PS1wt and PS1Δexon 10 and calculating the ratio of NTF/FL, we demonstrated that endoproteolysis of the PS1Δexon 10 molecule was ten-fold decreased compared to PS1wt (Fig. 1E). To address if this endoproteolytic pattern was due to a transiently overexpressed system, we also generated stable BD8 cell lines expressing PS1wt and PS1Δexon 10, respectively, and observed the same endoproteolytic pattern (data not shown). Thus, the large cytoplasmic loop seems to affect the rate of endoproteolysis of the PS1 molecule.

Next, we wanted to study the possibility that the removal of the loop had altered the topology of the PS1 molecule. Our group has previously shown that PS1 has nine TMDs (13), where the N-terminus is facing the

Downloaded from www.jbc.org at SMAC Consortium - University of Zürich, on March 14, 2011

cytosol and the C-terminus is facing the lumen. In order to determine the topology for the PS1Δexon 10 molecule we introduced a glycosylation acceptor site (Asn-Ser-Thr) in the C-terminal end. Glycosylation patterns for the transiently expressed constructs in BD8 cells were assessed by immunoblotting. The introduction of the glycosylation acceptor site resulted in a shift in migration for both the full-length PS1wt and PS1Δexon 10 (Fig. 1E, lane 4 & 8). Endoglycosidase H treatment reduced the size of the protein (Fig. 1F lane 5 & 9), confirming that the shift was caused by glycosylation and indicating that the C-terminus in the PS1Δexon 10 molecule had a luminal/extracellular orientation. Thus, the exon 10 deletion did not appear to induce an aberrant topology of the molecule.

The exon 10 coding region is vital for γ-secretase complex assembly and the complexes formed remain stable. To address if the apparent lower levels of NTFwt produced from PS1Δexon 10 is due to impaired endoproteolysis or if it is a consequence of less stable γ-secretase complexes, we generated a PS1 CTF construct lacking exon 10, CTF start 375 (Fig. 2A). When co-expressed with PS1 NTFwt in BD8 cells, thus bypassing endoproteolysis, we observed lower levels of NTFwt in the presence of CTF start 375 than in the presence of CTFwt. We also observed a lower expression level of NTFwt when using BD8 cells stably expressing NTFwt, BD8:NTF, (Fig. 2B). To analyze the stability of the complexes, we treated BD8:NTF cells expressing CTFwt and CTF start 375 molecules as well as BD8 cells expressing PS1Δexon 10 and PS1wt, with 50 μg/ml cycloheximide for different time points. We found that NTFwt co-expressed with CTF start 375 had a comparable half-life with NTFwt co-expressed with CTFwt, when monitoring between 1 hour to 16 hours (Fig. 2C). The same was observed for the PS1Δexon 10 molecule, which half-time was comparable with the PS1wt (Fig. 2D). This indicates that the loop is important for complex formation, since we still observed lowered NTF levels even under conditions bypassing PS endoproteolysis. The complexes formed from PS1 molecules lacking the loop remain as stable as wild type complexes.

PS1Δexon 10 affects Aβ formation but not AICD generation. Next, we wanted to assess the functional impact of PS1Δexon 10 on AICD and Aβ production. The PS1Δexon 10 molecule was transiently expressed in BD8 cells and γ-secretase activity was determined by monitoring AICD generation through the use of a luciferase reporter gene assay (32,33). Expression of PS1Δexon 10 did not reduce AICD generation compared to PS1wt when normalizing for protein expression (Fig. 3A). This finding is not compatible with *in vivo* data from Deng *et al.,* which indirectly showed a decreased AICD formation by demonstrating an accumulation of APP-CTF in the PS1Δexon 10 knock-in mice (29). However, when we also monitored NICD production we also found an unperturbed processing with the PS1Δexon 10 molecule (Fig. 3A).

Furthermore, we investigated the influence of PS1Δexon 10 on Aβ production by transfecting PS1wt or PS1Δexon 10 cDNA into BD8 cells stably expressing APPwt (BD8:APP). Sandwich immunoassay quantification revealed that the total Aβ production was strikingly impaired in cells transfected with PS1Δexon 10 compared to PS1wt (Fig. 3B). Importantly, the production of Aβ38, Aβ39 and Aβ40 was severely impaired, whereas the effect on Aβ42 generation was affected to a much lesser extent (Fig. 3C). Importantly, we observed the same production of Aβ40 when normalizing for NTF expression, indicating that the result is not due to lower levels of PS1 (Fig. 3D). Thus, the PS1Δexon 10 protein seems to affect Aβ40 generation more than Aβ42, similar to many PS1 FAD mutations (22,23). This also resulted in a 4.4 fold increase in the Aβ42/Aβ40 ratio for PS1Δexon 10 compared to PS1wt (Fig. 3E). This suggests that the large hydrophilic loop of PS1 affects ε/S3-site and γ-site cleavage differentially.

APP processing is affected when the last ten amino acids in the loop are removed. To assay how γ-secretase activity is affected by the absence of the loop under conditions bypassing endoproteolysis, we examined the impact of the CTF start 375 molecules on APP processing. We have previously shown that co-transfection of PS1 CTFwt and NTFwt can interact and restore γ-secretase activity in PS null cells (30). Using a luciferase reporter gene assay, we observed that co-expression of PS1

Downloaded from www.jbc.org at SMAC Consortium - University of Zürich, on March 14, 2011

NTFwt and CTF start 375 had the same effect on AICD formation as CTFwt and the PS1 lacking exon 10. Interestingly, the sandwich immunoassay also revealed a remarkably similar production pattern of different Aβ peptides as well as the total Aβ generation for the co-expressed NTFwt and CTF start 375 compared to the PS1Δexon 10 molecule (Fig. 4 *c.f.* Fig. 3).

To narrow down the region in exon 10 that is responsible for proper PS1 activity, we created an array of N-terminal truncated PS1 CTF molecules (Fig. 5A). When γ-secretase activity was assayed for these different truncated CTFs (expressed together with NTFwt) an unchanged activity at the ε-site (monitored by AICD formation) was observed for all truncations when normalizing for protein expression (Fig. 5B). However, a gradual decline in activity at the γ-site was seen paralleling the extent of truncation (Fig. 5C). The most dramatic shift in both activity and cleavage pattern could be seen between expressing CTF start 365 and CTF start 375 (Fig. 5D). Strikingly, the formation of Aβ42 was relatively unperturbed between the constructs, whereas expression of CTF start 375 resulted in a drastic decrease in formation of the shorter Aβ variants (Aβ40, Aβ39, Aβ38). Taken together, these results suggest that the loop domain controls the extent of Aβ formation, without affecting AICD production, and that the last C-terminal ten amino acids in the PS1 loop seems to differentially affect production of shorter Aβ variants.

DISCUSSION

PS is the catalytic moiety of the γ-secretase complex, which mediates both essential cell biological processes such as Notch receptor signaling, as well as cleavage of APP resulting in production of the AD-related Aβ-peptide. Despite its critical role in normal biology and pathobiology, the enzymatic mechanism underlying γ-secretase-mediated Notch and APP processing remains in large part elusive. To gain further insight into γ-secretase mediated catalysis, we have in this study focused on PS1. In particular, we concentrated our studies on the evolutionarily non-conserved hydrophilic loop, located between TMD6 and 7 in PS1, which has been suggested to be important for γ-secretase function. Our data show that this region plays a pivotal role for γ-secretase biology. First, the loop is required for efficient γ-secretase assembly and endoproteolysis. Second, it regulates γ-secretase activity differentially between the ε/S3-site and the γ-site. Third, the loop region is important for regulating Aβ production, where its absence causes a dramatic decrease in the formation of the shorter Aβ38, Aβ39 and Aβ40 isoforms and total Aβ released. Notably, the production of Aβ42 is only partially impaired under the same conditions. It is interesting to note that this effect on Aβ production resembles the Aβ phenotype of many FAD-linked PS1 mutants (22,23). Similar to the PS1Δexon 10 mutant, a total decrease in Aβ production, in combination with a less impaired Aβ42 generation, results in an increased Aβ42/Aβ1-X ratio for the FAD associated PS mutants. This Aβ-phenotype causes an enhanced amyloidosis in FAD as well as transgenic models harbouring FAD-linked PS. The FAD-like Aβ phenotype of PS1Δexon 10 also translates to increased amyloidosis, as recently demonstrated by Deng *et al* in transgenic mice (29).

The mechanism underlying FAD-linked production of different species (causing an increased Aβ42/ Aβ1-X ratio) is not known. One hypothesis, which has been raised, is that FAD-linked mutations give rise to a partial loss of function of the γ-secretase, which in turn causes a more severe effect on shorter Aβ peptides compared to the longer Aβ42 peptide. Our results are to some extent congruent with this hypothesis, since removal of the cytoplasmic loop causes a partial reduction in Aβ42, whereas the amount of the shorter secreted Aβ38, Aβ39 and Aβ40 peptides were decreased with 80% or more. Accordingly, our data would fit a partial loss of function model, except that the PS1Δexon 10 molecule is fully active at the ε/S3-site, which is not the case for most of PS FAD mutants. This suggests that PS1Δexon 10 γ-secretase processing is initiated by unperturbed ε-cleavage but gradually resulting in shorter peptides, especially beyond Aβ40. Several mechanisms could lead to a partial loss of γ-secretase processing. Our data show that the stability of the γ-secretase complex is not changed in the absence of the loop region, ruling out this

Downloaded from www.jbc.org at SMAC Consortium - University of Zürich, on March 14, 2011

mechanism as responsible for the impaired γ-secretase mediated APP processing.

We have previously shown that it is possible to reconstitute γ-secretase activity in the absence of PS endoproteolysis, by expressing PS NTF and CTF encoding constructs in PS null cells (30). This experimental paradigm enables a powerful system to study different domains and amino acids in PS for different aspects of PS biology. By utilizing this system we could observe that partial deletions of the loop region, from the N-terminal end to only a few amino acids remaining of the C-terminal end of the loop region, cause a progressive loss of both Aβ38, Aβ39 and Aβ40 as well as of Aβ42 production, which is in agreement with a gradual loss of function. Interestingly however, when removing the last C-terminal amino acids of the loop, Aβ42 production is not further impaired, whereas the production of Aβ38-40 is dramatically lowered. Thus, it appears that the C-terminal amino acids of exon 10 are more important for Aβ38-40 production than for Aβ42. These data also implicate that the differential effect on Aβ42 versus shorter Aβ peptides could not solely be explained by a general loss of function, since we would then have expected a concomitant lowering in Aβ42 and AICD upon removing the most C-terminal amino acids.

We do not currently understand why this region has a differential effect on Aβ peptide production, but the primary structure may be important. This is supported by the observation that expression of full-length Δexon 10 results in the same phenotype as expression of NTFwt and CTF start 375: endoproteolysis of Δexon 10 results in a CTF with an extension of 20 N-terminal amino acids (residues 300-320; encoded by exon 9). Although the removal of Δexon 10 results in an Aβ phenotype similar to many FAD mutants, no FAD causing mutation has so far been identified in this region. Irrespective of the relationship between Aβ42 and the shorter peptides, the present study and the data on FAD mutants suggest that Aβ42 production in particular seems to be less sensitive to genetic modifications of the presenilin gene. Indeed, in efforts identifying amino acids critical for inhibition by γ-secretase-directed small molecules, Basi and colleagues made a similar observation, i.e. that many artificial mutants cause a more severe loss of shorter Aβ variants than Aβ42 (40). Future studies are warranted to explain the differential sensitivity of PS mutations on Aβ42 production versus other shorter Aβ peptides.

Since many studies have pointed out the importance of sustaining the Notch signaling pathway in adulthood (9-12), the differences in Notch S3-site/ APP ε-site and APP γ-site processing that we observe in the absence of the loop is of great interest. One reason for the different cleavage activity observed could be due to a structural change in the docking or the active site. The removal of the loop may induce an altered topography in these sites, leading to a weaker binding to the substrates. Indeed, Kornilova et al have shown that PS FAD mutations have reduced photolabeling by a transition-state analogue (41). Moreover, Berezovska and colleagues have published two reports that show the influence of both genetic and pharmacological manipulations, which increase the Aβ42/Aβ40 ratio, to be associated with a uniformal conformational change in the catalytic site of PS1 (42,43). Our data using a biotin-labeled transition-state analogue inhibitor of γ-secretase show a trend of less binding (15-70% reduction) of PS1Δexon 10-NTF compared to PS1wt-NTF when normalizing for their corresponding input NTF's. This implicates that the active site of PS1Δexon 10 has a more close conformation than the PS1 wt. It remains to be established whether the loop region is critical for the activity of γ-secretase modulators (GSM). Thus, the loop can be important for the positioning of the substrates but that the initial processing at the ε/S3- site is not affected, whereas a gradually decrease occurs in the processing towards shorter peptides.

In conclusion, the data presented here suggest that the production of Aβ42 is distinct from Aβ38, Aβ39 and Aβ40, and that the integrity of the large hydrophilic loop between TMD 6 and 7 of PS1 is important for proper γ-secretase complex assembly, PS1 endoproteolysis and determination of Aβ peptide profiles. The large hydrophilic loop does not however affect the AICD or NICD production. This result is of importance, since avoiding Notch processing is a prerequisite when designing drugs that target the γ-secretase complex in the treatment of AD.

Downloaded from www.jbc.org at SMAC Consortium - University of Zürich, on March 14, 2011

REFERENCES

1. Glenner, G. G., and Wong, C. W. (1984) *Biochem Biophys Res Commun* **122**, 1131-1135
2. Nukina, N., and Ihara, Y. (1986) *J Biochem* **99**, 1541-1544
3. Esler, W. P., and Wolfe, M. S. (2001) *Science* **293**, 1449-1454
4. Brown, M. S., Ye, J., Rawson, R. B., and Goldstein, J. L. (2000) *Cell* **100**, 391-398
5. Francis, R., McGrath, G., Zhang, J., Ruddy, D. A., Sym, M., Apfeld, J., Nicoll, M., Maxwell, M., Hai, B., Ellis, M. C., Parks, A. L., Xu, W., Li, J., Gurney, M., Myers, R. L., Himes, C. S., Hiebsch, R., Ruble, C., Nye, J. S., and Curtis, D. (2002) *Dev Cell* **3**, 85-97
6. Goutte, C., Tsunozaki, M., Hale, V. A., and Priess, J. R. (2002) *Proc Natl Acad Sci U S A* **99**, 775-779
7. Wolfe, M. S., Xia, W., Ostaszewski, B. L., Diehl, T. S., Kimberly, W. T., and Selkoe, D. J. (1999) *Nature* **398**, 513-517
8. Yu, G., Nishimura, M., Arawaka, S., Levitan, D., Zhang, L., Tandon, A., Song, Y. Q., Rogaeva, E., Chen, F., Kawarai, T., Supala, A., Levesque, L., Yu, H., Yang, D. S., Holmes, E., Milman, P., Liang, Y., Zhang, D. M., Xu, D. H., Sato, C., Rogaev, E., Smith, M., Janus, C., Zhang, Y., Aebersold, R., Farrer, L. S., Sorbi, S., Bruni, A., Fraser, P., and St George-Hyslop, P. (2000) *Nature* **407**, 48-54
9. Hyde, L. A., McHugh, N. A., Chen, J., Zhang, Q., Manfra, D., Nomeir, A. A., Josien, H., Bara, T., Clader, J. W., Zhang, L., Parker, E. M., and Higgins, G. A. (2006) *J Pharmacol Exp Ther* **319**, 1133-1143
10. Milano, J., McKay, J., Dagenais, C., Foster-Brown, L., Pognan, F., Gadient, R., Jacobs, R. T., Zacco, A., Greenberg, B., and Ciaccio, P. J. (2004) *Toxicol Sci* **82**, 341-358
11. Searfoss, G. H., Jordan, W. H., Calligaro, D. O., Galbreath, E. J., Schirtzinger, L. M., Berridge, B. R., Gao, H., Higgins, M. A., May, P. C., and Ryan, T. P. (2003) *J Biol Chem* **278**, 46107-46116
12. Wong, G. T., Manfra, D., Poulet, F. M., Zhang, Q., Josien, H., Bara, T., Engström, L., Pinzon-Ortiz, M., Fine, J. S., Lee, H. J., Zhang, L., Higgins, G. A., and Parker, E. M. (2004) *J Biol Chem* **279**, 12876-12882
13. Laudon, H., Hansson, E. M., Melen, K., Bergman, A., Farmery, M. R., Winblad, B., Lendahl, U., von Heijne, G., and Näslund, J. (2005) *J Biol Chem* **280**, 35352-35360
14. Henricson, A., Kall, L., and Sonnhammer, E. L. (2005) *FEBS J* **272**, 2727-2733
15. Spasic, D., Tolia, A., Dillen, K., Baert, V., De Strooper, B., Vrijens, S., and Annaert, W. (2006) *J Biol Chem* **281**, 26569-26577
16. Dillen, K., and Annaert, W. (2006) *Int Rev Cytol* **254**, 215-300
17. Thinakaran, G., Borchelt, D. R., Lee, M. K., Slunt, H. H., Spitzer, L., Kim, G., Ratovitsky, T., Davenport, F., Nordstedt, C., Seeger, M., Hardy, J., Levey, A. I., Gandy, S. E., Jenkins, N. A., Copeland, N. G., Price, D. L., and Sisodia, S. S. (1996) *Neuron* **17**, 181-190
18. Czirr, E., Cottrell, B. A., Leuchtenberger, S., Kukar, T., Ladd, T. B., Esselmann, H., Paul, S., Schubenel, R., Torpey, J. W., Pietrzik, C. U., Golde, T. E., Wiltfang, J., Baumann, K., Koo, E. H., and Weggen, S. (2008) *J Biol Chem* **283**, 17049-17054
19. Kakuda, N., Funamoto, S., Yagishita, S., Takami, M., Osawa, S., Dohmae, N., and Ihara, Y. (2006) *J Biol Chem* **281**, 14776-14786

Downloaded from www.jbc.org at SMAC Consortium - University of Zürich, on March 14, 2011

20. Qi-Takahara, Y., Morishima-Kawashima, M., Tanimura, Y., Dolios, G., Hirotani, N., Horikoshi, Y., Kametani, F., Maeda, M., Saido, T. C., Wang, R., and Ihara, Y. (2005) *J Neurosci* **25**, 436-445
21. Shankar, G. M., Li, S., Mehta, T. H., Garcia-Munoz, A., Shepardson, N. E., Smith, I., Brett, F. M., Farrell, M. A., Rowan, M. J., Lemere, C. A., Regan, C. M., Walsh, D. M., Sabatini, B. L., and Selkoe, D. J. (2008) *Nat Med* **14**, 837-842
22. Bentahir, M., Nyabi, O., Verhamme, J., Tolia, A., Horre, K., Wiltfang, J., Esselmann, H., and De Strooper, B. (2006) *J Neurochem* **96**, 732-742
23. Kumar-Singh, S., Theuns, J., Van Broeck, B., Pirici, D., Vennekens, K., Corsmit, E., Cruts, M., Dermaut, B., Wang, R., and Van Broeckhoven, C. (2006) *Hum Mutat* **27**, 686-695
24. De Strooper, B. (2007) *EMBO Rep* **8**, 141-146
25. Wolfe, M. S. (2007) *EMBO Rep* **8**, 136-140
26. Strömberg, K., Hansson, E. M., Laudon, H., Bergstedt, S., Näslund, J., Lundkvist, J., and Lendahl, U. (2005) *J Neurochem* **95**, 880-890
27. Xia, X., Wang, P., Sun, X., Soriano, S., Shum, W. K., Yamaguchi, H., Trumbauer, M. E., Takashima, A., Koo, E. H., and Zheng, H. (2002) *Proc Natl Acad Sci U S A* **99**, 8760-8765
28. Saura, C. A., Tomita, T., Soriano, S., Takahashi, M., Leem, J. Y., Honda, T., Koo, E. H., Iwatsubo, T., and Thinakaran, G. (2000) *J Biol Chem* **275**, 17136-17142
29. Deng, Y., Tarassishin, L., Kallhoff, V., Peethumnongsin, E., Wu, L., Li, Y. M., and Zheng, H. (2006) *J Neurosci* **26**, 3845-3854
30. Laudon, H., Mathews, P. M., Karlström, H., Bergman, A., Farmery, M. R., Nixon, R. A., Winblad, B., Gandy, S. E., Lendahl, U., Lundkvist, J., and Näslund, J. (2004) *J Neurochem* **89**, 44-53
31. Farmery, M. R., Tjernberg, L. O., Pursglove, S. E., Bergman, A., Winblad, B., and Näslund, J. (2003) *J Biol Chem* **278**, 24277-24284
32. Taniguchi, Y., Karlström, H., Lundkvist, J., Mizutani, T., Otaka, A., Vestling, M., Bernstein, A., Donoviel, D., Lendahl, U., and Honjo, T. (2002) *Proc Natl Acad Sci U S A* **99**, 4014-4019
33. Karlström, H., Bergman, A., Lendahl, U., Näslund, J., and Lundkvist, J. (2002) *J Biol Chem* **277**, 6763-6766
34. Donoviel, D. B., Hadjantonakis, A. K., Ikeda, M., Zheng, H., Hyslop, P. S., and Bernstein, A. (1999) *Genes Dev* **13**, 2801-2810
35. Bergman, A., Laudon, H., Winblad, B., Lundkvist, J., and Näslund, J. (2004) *J Biol Chem* **279**, 45564-45572
36. Teranishi, Y., Hur, J. Y., Welander, H., Frånberg, J., Aoki, M., Winblad, B., Frykman, S., and Tjernberg, L. O. (2009) *J Cell Mol Med*
37. Bergman, A., Hansson, E. M., Pursglove, S. E., Farmery, M. R., Lannfelt, L., Lendahl, U., Lundkvist, J., and Näslund, J. (2004) *J Biol Chem* **279**, 16744-16753
38. Steiner, H., Romig, H., Pesold, B., Philipp, U., Baader, M., Citron, M., Loetscher, H., Jacobsen, H., and Haass, C. (1999) *Biochemistry* **38**, 14600-14605
39. Podlisny, M. B., Citron, M., Amarante, P., Sherrington, R., Xia, W., Zhang, J., Diehl, T., Levesque, G., Fraser, P., Haass, C., Koo, E. H., Seubert, P., St George-Hyslop, P., Teplow, D. B., and Selkoe, D. J. (1997) *Neurobiol Dis* **3**, 325-337
40. Zhao, B., Yu, M., Neitzel, M., Marugg, J., Jagodzinski, J., Lee, M., Hu, K., Schenk, D., Yednock, T., and Basi, G. (2008) *J Biol Chem* **283**, 2927-2938
41. Kornilova, A. Y., Bihel, F., Das, C., and Wolfe, M. S. (2005) *Proc Natl Acad Sci U S A* **102**, 3230-3235

Downloaded from www.jbc.org at SMAC Consortium - University of Zürich, on March 14, 2011

42. Berezovska, O., Lleo, A., Herl, L. D., Frosch, M. P., Stern, E. A., Bacskai, B. J., and Hyman, B. T. (2005) *J Neurosci* **25**, 3009-3017
43. Uemura, K., Lill, C. M., Li, X., Peters, J. A., Ivanov, A., Fan, Z., DeStrooper, B., Bacskai, B. J., Hyman, B. T., and Berezovska, O. (2009) *PLoS One* **4**, e7893

FOOTNOTES

We gratefully thank Dr. P. M. Mathews for providing the NT1 antibody. We are also grateful to Dr. E. Benedikz for the APPwt construct and Drs. Donoviel and St. George-Hyslop for the gift of the PS1/2-deficient BD8 cells. We thank as well M.P. Lewin and F. Olsson at AstraZeneca for excellent technical assistance.

This work was supported by grants from Swedish Brain Power, Wallenberg Stiftelsen, Loo och Hans Ostermans Stiftelse, Magnus Bergvalls Stiftlelse, Fonden för Ålderforskning vid Karolinska Institutet, Stiftelsen för Gamla Tjänarinnor and Gun och Bertil Stohnes Stiftelse.

FIGURE LEGENDS

Fig. 1. PS1 lacking exon 10 shows impaired endoproteolysis but forms complexes with other γ -secretase subunits. (A) Schematic presentation of PS1wt and the PS1Δexon 10, lacking amino acids 320 to 374. Arrowhead depicts the endoproteolytic site. (B) Western blot analysis of lysates from BD8 cells expressing PS1wt and PS1Δexon 10 using a PS1-NTF antibody (NT-1). (C) Co-immunoprecipitation of BD8 lysats expressing PS1wt and PS1Δexon 10 using two different capture antibodies; N1660 (raised against Nicastrin) and O2C2 (raised against Aph-1aL). Detection was performed with PS1-NTF antibody (NT-1) and Pen-2 (3981), respectively. § indicate an unspecific band and # indicate the IgG band. (D) GCB pulldown of BD8 cells stably expressing PS1wt or PS1Δexon 10. Western blot were analyzed for NTF expression with a PS1-NTF antibody (NT-1) (E) Quantification of the endoproteolysed forms (NTF) versus full-length forms (FL) from seven Western blots with lysed BD8 cells expressing PS1wt and PS1Δexon 10. The Western blots were probed with a PS1-NTF antibody (NT-1) and quantified with a CCD camera. The ratio NTF/FL from PS1wt was set to 1. (F) EndoH treatment of BD8 cells expressing PS1wt, PS1wt optC, PS1Δexon 10 and PS1Δexon 10 optC, using a PS1-NTF antibody (NT-1), shows that PS1Δexon 10 has a normal nine transmembrane topology. *Error bars* indicate the S.D., and statistical significance is calculated by the non-parametric Mann-Whitney U test. *, $p < 0.05$; **, $p < 0.01$; ***, $p < 0.001$.

Fig. 2. The exon 10 region is important for efficient γ-secretase complex formation but does not affect the stability of formed complexes. (A) Schematic presentation of the CTF construct lacking exon 10, CTF start 375. (B) Expression analysis of lysed BD8 or BD8:NTF cells transfected with PS1wt, PS1Δexon 10, CTFwt, CTF start 375 and empty vector, respectively, using a PS1-NTF antibody (NT-1). A β-actin antibody was used to ensure equal amounts of loaded protein. (C, D) BD8:NTF cells transfected with CTF wt, CTF start 375 and empty vector and BD8 cells expressing PS1wt and PS1Δexon 10, respectively, were treated with cycloheximide (50 μg/ml) for seven different time points between 0 hours and 16 hours. Lysates were analyzed for NTF expression with a PS1-NTF antibody (NT-1). A β-actin antibody was used to ensure equal amounts of loaded protein.

Fig. 3. PS1 lacking exon 10 possesses a differential loss of function on AICD and Aβ formation. (A) Lysats from BD8 cells expressing PS1wt and PS1Δexon 10 were monitored with a luciferase reporter gene assay for AICD and NICD production, using transiently transfected C99-GVP/NotchΔE-GVP, MH100 and CMV-β-gal constructs. Luciferase activity

Downloaded from www.jbc.org at SMAC Consortium - University of Zürich, on March 14, 2011

was normalized for protein expression (right panel) and transfection efficiency. PS1wt was set to 100% AICD formation. The right panel is a representative western blot from four independent experiments, using a PS1-NTF antibody (NT-1). (B) Sandwich immunoassay was used for detection of secreted total Aβ production using 4G8 and 6E10 antibodies. Total Aβ was set to 100% for PS1wt. (C) Detection of secreted Aβ38, Aβ39, Aβ40 and Aβ42 using 6E10 or C-terminal specific Aβ40/38/42 antibodies as a capture antibody and Aβ39, Aβ40, Aβ42 and/ or 6E10 specific antibodies for detection. Levels of Aβ38, Aβ39, Aβ40 and Aβ42 for PS1wt were set to 100%, respectively. # indicate that the peptide were below detection limit regarding the standard curve, but <10% of wt. (D) When secreted Aβ40 was normalized for protein expression (right panel), the same production was observed as in C. The right panel is a representative western blot from four independent experiments, using a PS1-NTF antibody (NT-1). (E) Aβ42/Aβ40 ratio of PS1wt and PS1Δexon 10. *Error bars* indicate the S.D., and statistical significance is calculated by the non-parametric Mann-Whitney U test. *, p <0.05; **, p <0.01; ***, p <0.001.

Fig. 4. The exon 10 encoding region of PS1 has no effect on AICD production but a direct effect on Aβ generation. (A) Luciferase reporter gene assay monitoring AICD generation in BD8 cells expressing the CTFwt or CTF start 375 molecules together with NTFwt, C99-GVP, MH100 and CMV-β-gal constructs. Luciferase activity was normalized for transfection efficiency using a β-galactosidase assay and protein expression (right panel). NTFwt + CTFwt was set to 100% AICD formation. The right panel is a representative western blot from four independent experiments, using a PS1-NTF antibody (NT-1). (B) Sandwich immunoassay was used for detection of secreted total Aβ production using 4G8 and 6E10 antibodies. Total Aβ was set to 100% for NTFwt + CTFwt. (C) Detection of secreted Aβ38, Aβ39, Aβ40 and Aβ42 using 6E10 or C-terminal specific Aβ40/38/42 antibodies as a capture antibody and Aβ39, Aβ40, Aβ42 and/ or 6E10 specific antibodies for detection. Levels of Aβ38, Aβ39, Aβ40 and Aβ42 for NTFwt + CTFwt were set to 100%, respectively. # indicate that the peptide were below detection limit regarding the standard curve, but <10% of wt. (D) When secreted Aβ40 was normalized for protein expression (right panel), the same production was observed as in C. The right panel is a representative western blot from four independent experiments, using a PS1-NTF antibody (NT-1). (E) Aβ42/Aβ40 ratio of CTFwt and CTF start 375 with NTFwt. *Error bars* indicate the S.D., and statistical significance is calculated by the non-parametric Mann-Whitney U test. *, p <0.05; **, p <0.01; ***, p <0.001.

Fig. 5. The ten most C-terminal amino acids encoded by exon 10 are important for regulating the Aβ profile. (A) Schematic presentation of the various N-terminal truncated CTF molecules. (B) Luciferase reporter gene assay monitoring AICD generation in BD8 cells expressing all CTF molecules together with NTFwt, C99-GVP, MH100 and CMV-β-gal constructs. Luciferase activity was normalized for transfection efficiency using a β-galactosidase assay and protein expression (lower panel). NTFwt + CTFwt was set to 100% AICD formation. The lower panel is a representative western blot from four independent experiments, using a PS1-NTF antibody (NT-1). (C) Sandwich immunoassay was used for detection of secreted total Aβ production using 4G8 and 6E10 antibodies. Total Aβ was set to 100% for NTFwt + CTFwt. (D) Detection of secreted Aβ38, Aβ39, Aβ40 and Aβ42 using 6E10 or C-terminal specific Aβ40/38/42 antibodies as a capture antibody and Aβ39, Aβ40, Aβ42 and/ or 6E10 specific antibodies for detection. Levels of Aβ38, Aβ39, Aβ40 and Aβ42 for NTFwt + CTFwt were set to 100%, respectively. # indicate that the peptide were below detection limit regarding the standard curve, but <10% of wt. (E) When secreted Aβ40 was normalized for protein expression (lower panel), the same production was observed as in D.

Downloaded from www.jbc.org at SMAC Consortium - University of Zürich, on March 14, 2011

The lower panel is a representative western blot from four independent experiments, using a PS1-NTF antibody (NT-1). (F) Aβ42/Aβ40 ratio of all CTF molecules with NTFwt. *Error bars* indicate the S.D., and statistical significance is calculated by the non-parametric Mann-Whitney U test. *, $p < 0.05$; **, $p < 0.01$; ***, $p < 0.001$.

Downloaded from www.jbc.org at SMAC Consortium - University of Zürich, on March 14, 2011

Figure 1

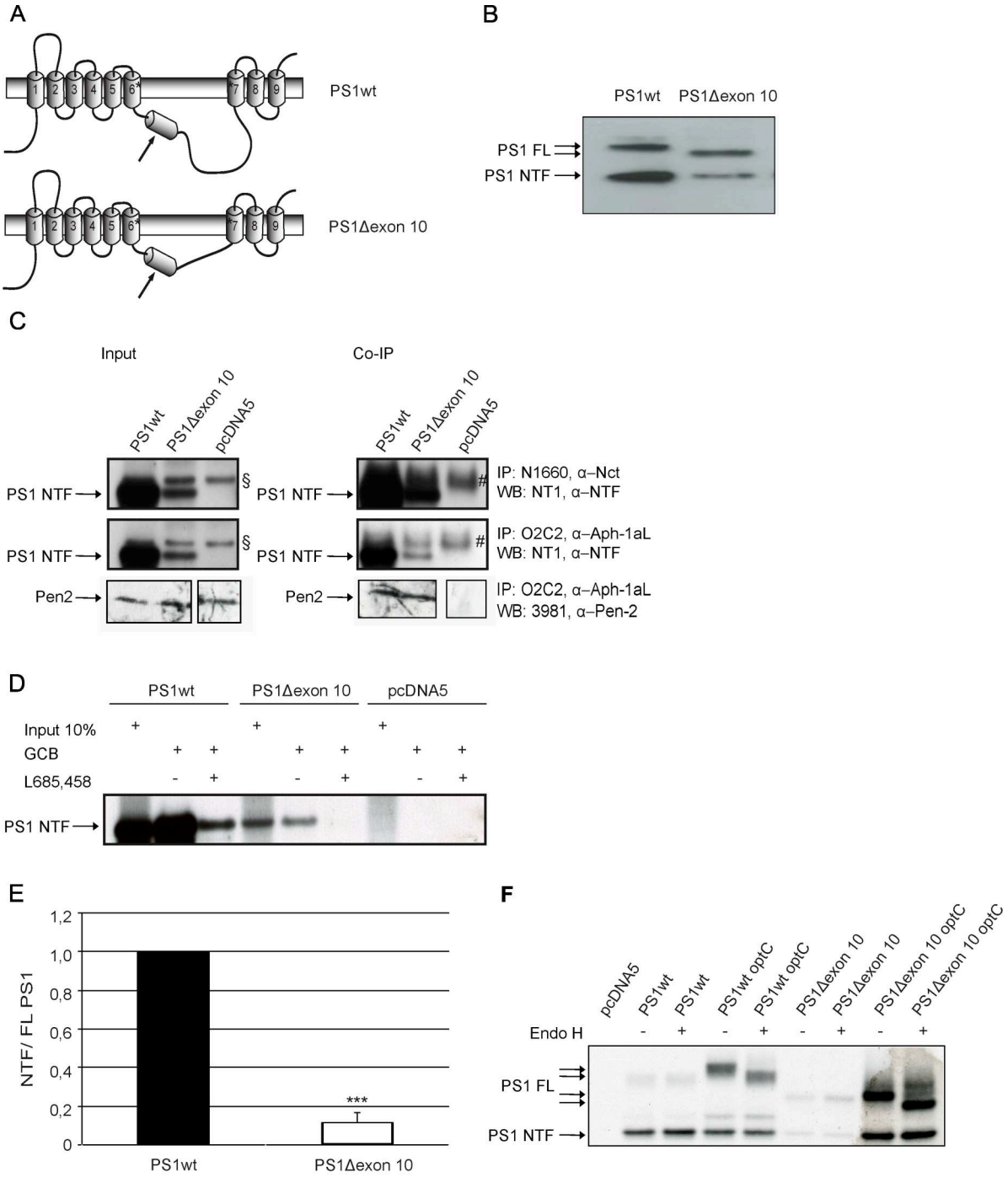

Downloaded from www.jbc.org at SMAC Consortium - University of Zürich, on March 14, 2011

Figure 2

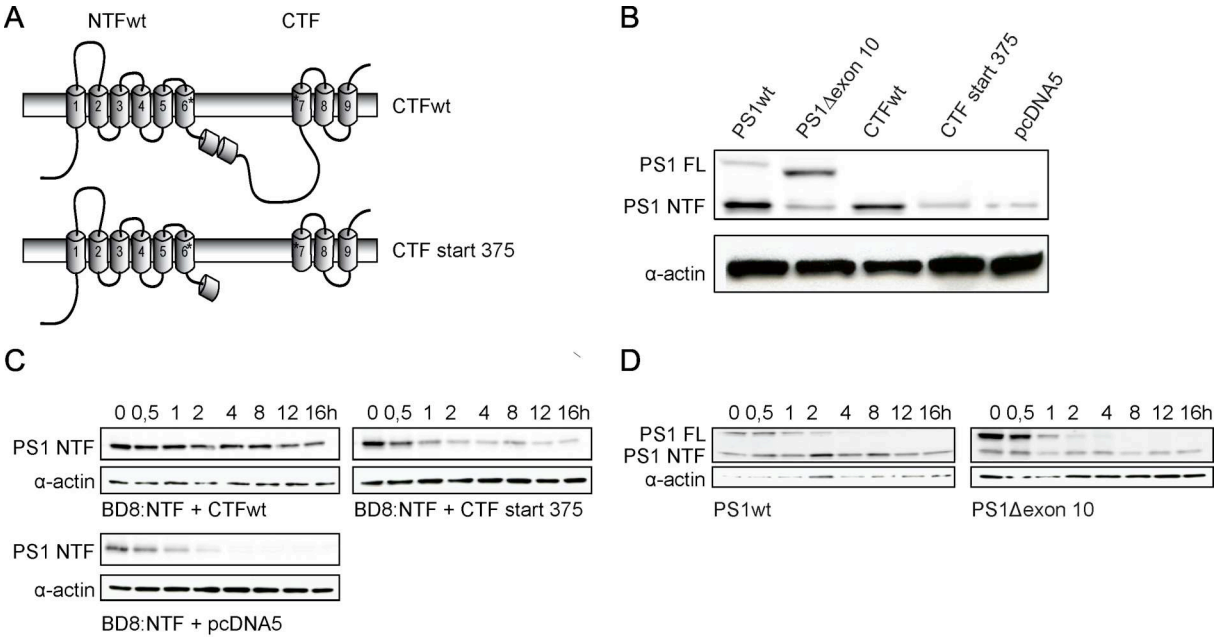

Downloaded from www.jbc.org at SMAC Consortium - University of Zürich, on March 14, 2011

Figure 3

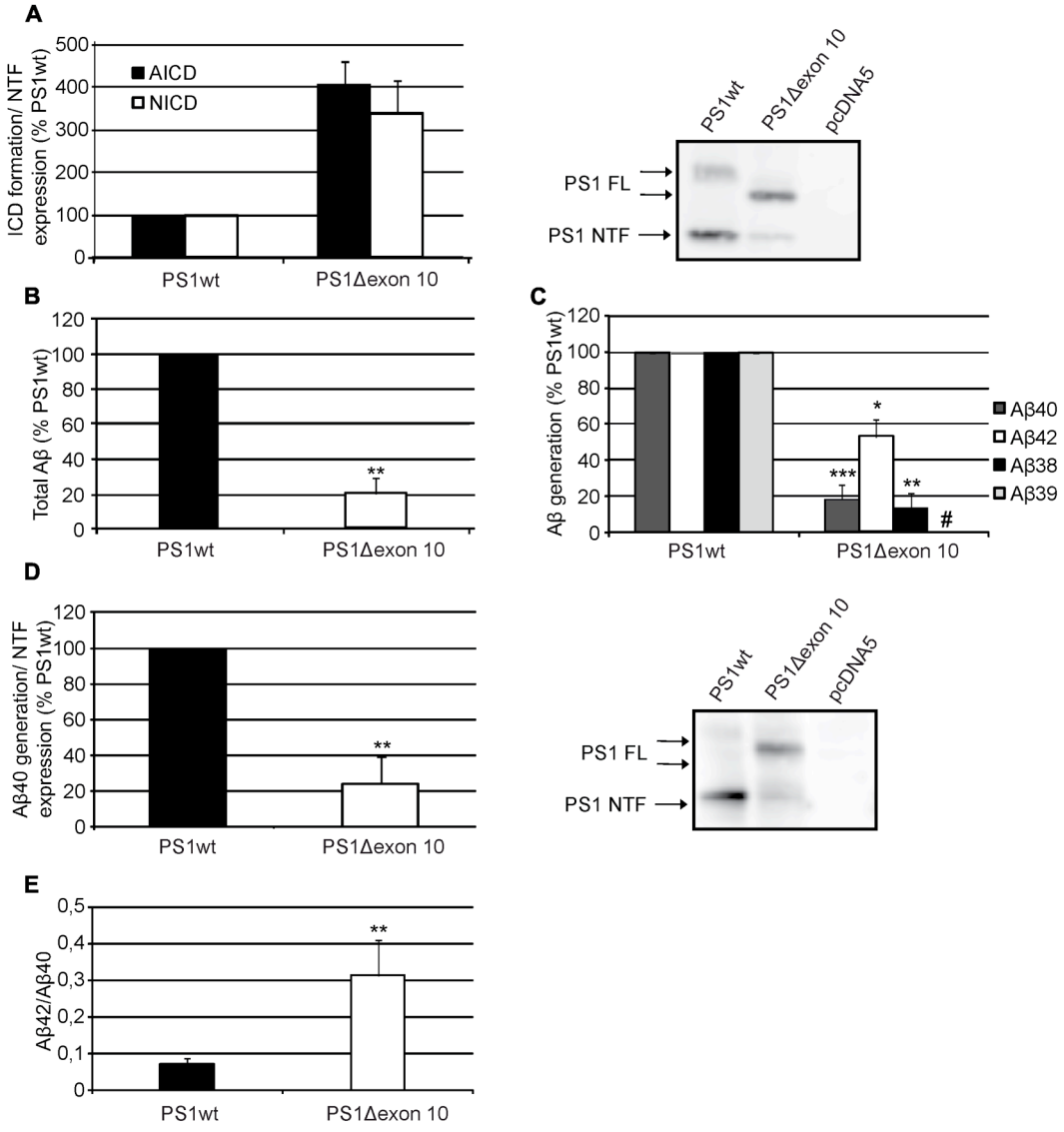

Downloaded from www.jbc.org at SMAC Consortium - University of Zürich, on March 14, 2011

Figure 4

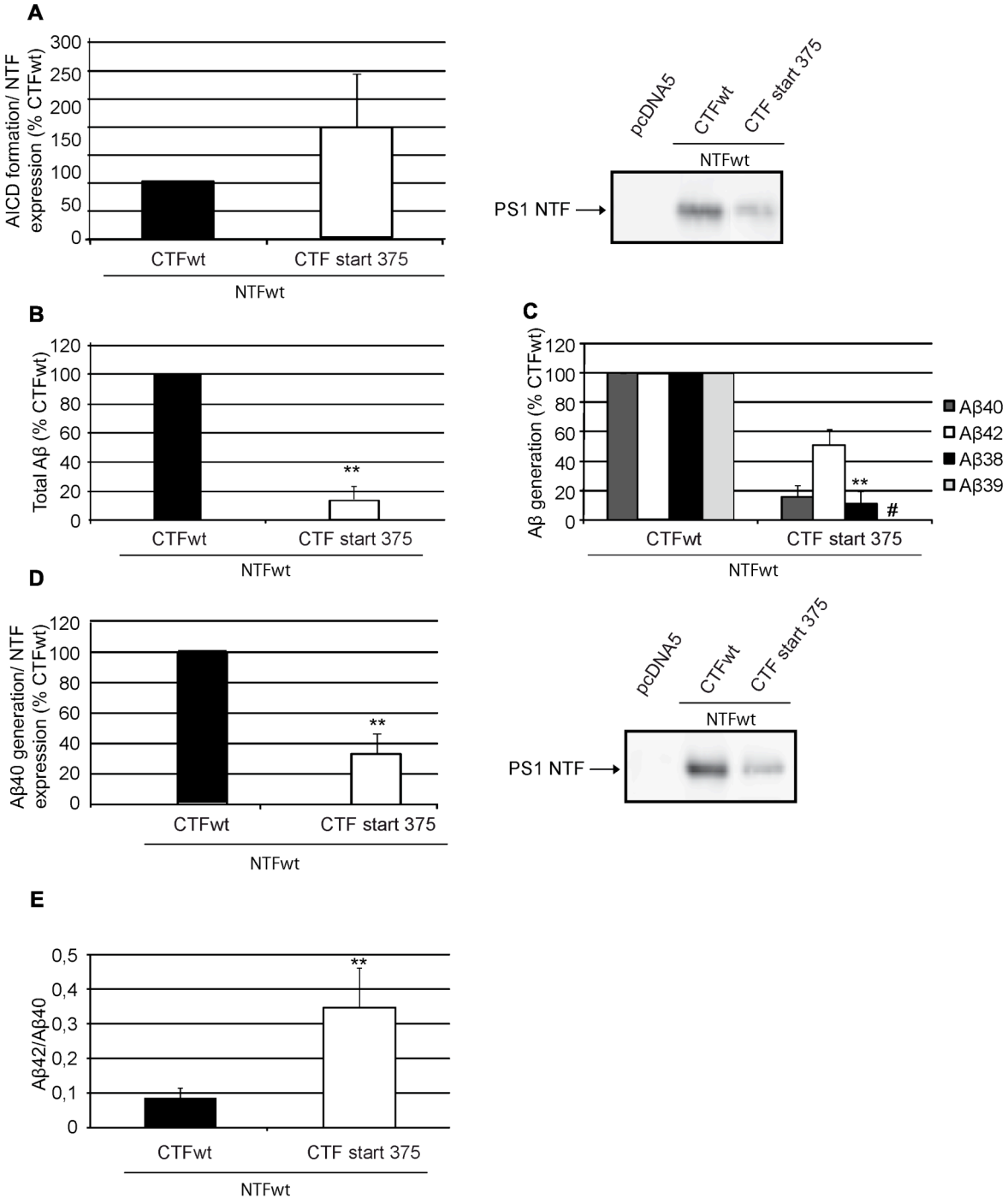

Downloaded from www.jbc.org at SMAC Consortium - University of Zürich, on March 14, 2011

Figure 5

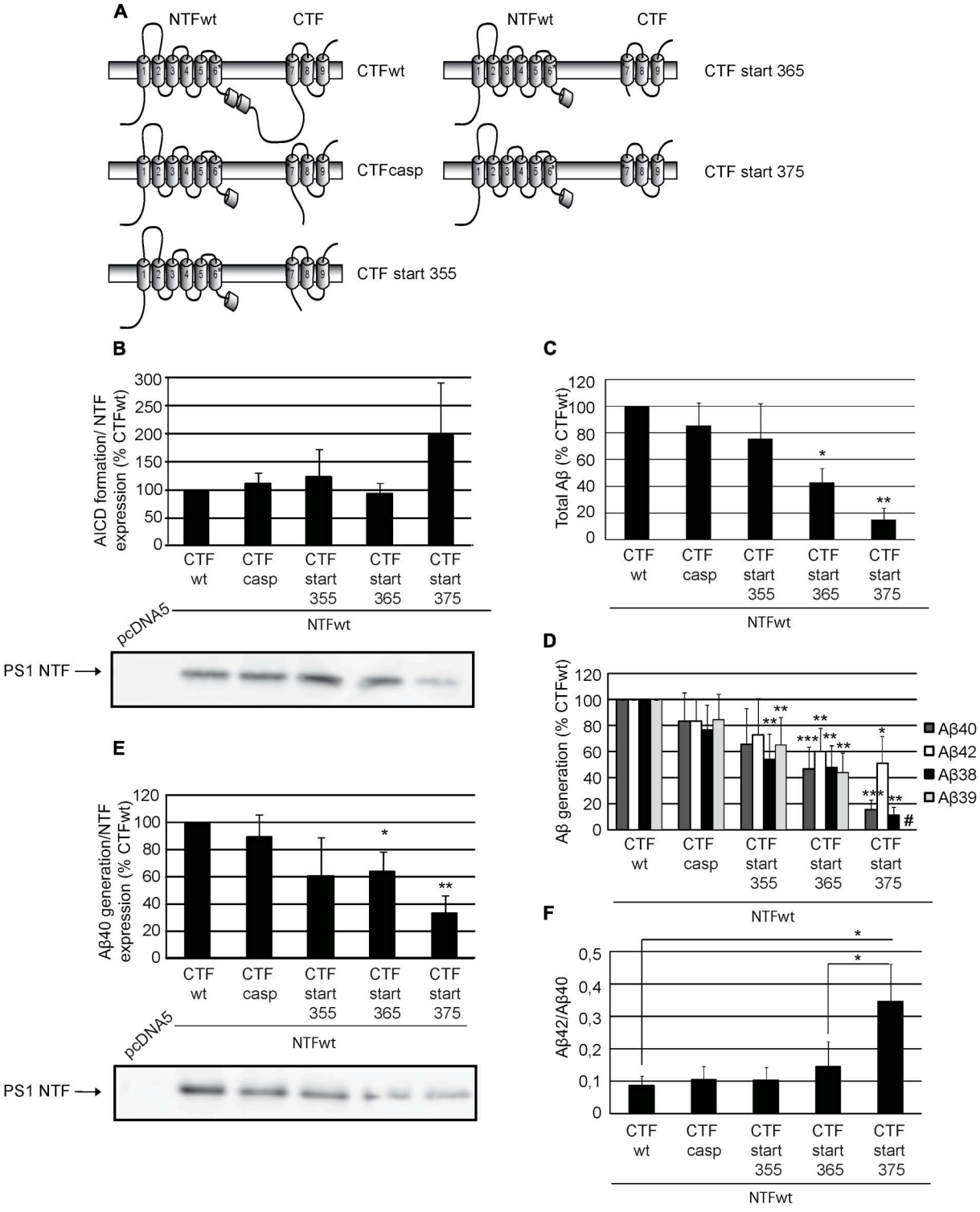

Downloaded from www.jbc.org at SMAC Consortium - University of Zürich, on March 14, 2011